Accepted Manuscript

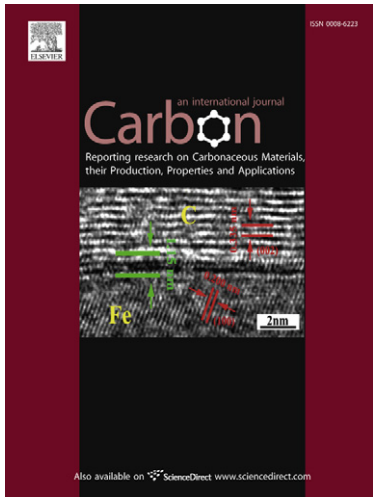

Development of stiff, strong, yet tough composites by the addition of solvent exfoliated graphene to polyurethane

Umar Khan, Peter May, Arlene O'Neill, Jonathan N Coleman

PII: S0008-6223(10)00501-4
DOI: 10.1016/j.carbon.2010.07.008
Reference: CARBON 6010

To appear in: *Carbon*

Received Date: 28 May 2010
Accepted Date: 6 July 2010

Please cite this article as: Khan, U., May, P., O'Neill, A., Coleman, J.N., Development of stiff, strong, yet tough composites by the addition of solvent exfoliated graphene to polyurethane, *Carbon* (2010), doi: 10.1016/j.carbon.2010.07.008

Development of stiff, strong, yet tough composites by the addition of solvent exfoliated graphene to polyurethane

Umar Khan, Peter May, Arlene O'Neill and Jonathan N Coleman*

School of Physics and CRANN, Trinity College Dublin, Dublin 2, Ireland

Abstract

We have prepared graphene dispersions, stabilised by polyurethane in tetrahydrofuran and dimethylformamide. These dispersions can be drop-cast to produce free-standing composite films. The graphene mass fraction is determined by the concentration of dispersed graphene and can be controllably varied from 0% to 90%. Raman spectroscopy and Helium ion microscopy show the graphene to well-dispersed and well-exfoliated in the composites, even at mass fractions of 55%. On addition of graphene, the Young's modulus and stress at 3% strain increase by ×100, saturating at 1 GPa and 25 MPa respectively for mass fractions above 50wt%. While the ultimate tensile strength does not vary significantly with graphene content, the strain at break and toughness degrade heavily on graphene addition. Both these properties fall by ×1000 as the graphene content is increased to 90wt%. However, the rate of increase of Young's modulus and stress at 3% strain with mass fraction is greater than the rate of decrease of ductility and toughness. This makes it possible to prepare composites with high modulus, stress at low strain and ultimate tensile strength as well as relatively high toughness and ductility. This could lead to new materials that are stiff, strong and tough.

* Corresponding author. Fax: ++353 1 6711759. Email address: colemaj@tcd.ie (J.N. Coleman)

1.0 Introduction

Since the demonstration of liquid phase exfoliation of graphene oxide[1, 2] and later of pristine graphene[3-5], it has been clear that such materials have huge potential as fillers in composites or hybrids[1]. The fact that graphene displays both the highest stiffness and strength of any material known to man[6] suggests that it should be very promising as a reinforcing filler in polymer-based composites. However, a number of papers have appeared on this subject, generally describing the reinforcement of rigid thermoplastics, with none showing outstanding results.[7-15] In general, the increases in stiffness have been moderate, typically by less than a factor of 3. We can quantify the reinforcement as the rate of increase in modulus with respect to graphene volume fraction, dY/dV_f.[16] From the rule of mixtures we would expect dY/dV_f for graphene-filled thermoplastics to approach the graphene modulus, i.e. 1TPa. However, the best results in the literature are equivalent to dY/dV_f ~110 GPa.[14] In comparison, dY/dV_f values in excess of 1 TPa have been observed for polymer-nanotube composites.[16] Young et al have shown (for graphene-PMMA composites at least), that this poor performance is due to very poor stress-transfer at the interface.[17] This is different to polymer-nanotube composites where good stress transfer has been observed by many researchers.[18, 19] In principle, stress transfer can be improved by functionalisation. However, a number of authors have attempted this without great success.[8, 13] These considerations cast doubt on the hopes of many, that graphene will play an important role in composites for mechanical applications.

With this in mind, we propose a different approach. Rather than reinforcing thermoplastics, we suggest that graphene might make an impact reinforcing elastomers. Reinforcement mechanisms in elastomeric composites are more complex than in thermoplastic based composites, a fact that may circumvent the poor stress transfer described above. Hard thermoplastics are characterised by relatively high stiffness and strength but low

ductility and toughness (work done to fracture). Conversely, elastomers are characterised by low stiffness and low stress at low strain but high ductility and toughness. We propose that addition of graphene to elastomers could result in a material with positive elements of both hard thermoplastics and elastomers: high stiffness and strength yet relatively large ductility and toughness. Such materials would be useful in a range of applications.

For such composites to have the properties outlined, a delicate balance must be maintained. While addition of nano-fillers such as nanotubes, nanoclays, nanofibres etc to elastomers may result in increases in strength and stiffness, this is usually accompanied by reduction in ductility and toughness.[20-23] Thus, it will be critical to improve stiffness and strength at a faster rate than ductility and toughness are degraded. This has been attempted before by filling polyurethane (PU) with nanotubes.[20, 24] Significant increases in stiffness and strength were observed but at a cost of very large decreases in ductility and toughness. The result was nanotube-reinforced PU which was mechanically, slightly inferior to a typical thermoplastic. In addition, composites have been prepared of polyurethane filled with graphene oxide and functionalised graphene.[25-28] However, it would be simpler to prepare composites from pristine graphene, exfoliated from liquids.[3, 4] This material is largely defect free and requires no acid treatment or chemical reduction during synthesis.

In this work we show that liquid exfoliated graphene is a very promising filler for reinforcement of elastomers than carbon nanotubes. We have used liquid exfoliated graphene to prepare PU-graphene composites with graphene mass fractions of up to 90%. The graphene remains exfoliated and is reasonably well dispersed even at high mass fractions. Thermal measurements show the graphene to interact strongly with the PU soft segments. We observed exponential increases in modulus and stress at low strain with mass fraction. Critically, we observed a slower exponential decrease in ductility and toughness. The ultimate tensile strength remained reasonably constant over a wide range of mass fractions.

This allowed us to prepare composites with modulus, strength and stress at low strain typical of hard thermoplastics but with high ductility and toughness.

2.0 Methods

Graphite Flakes (Sigma Aldridge) were dispersed in DMF (initial concentration 3 mg/ml) in a sonic bath (Branson MT-1510, 80Watt) for 150hrs. While we appreciate that this results in a very long sonication time, we are working on alternative preparation methods which will give much shorter sonication times. The dispersion was split into two portions which were centrifuged at 500 rpm for 22.5 and 45 minutes and two other portions centrifuged at 750 and 1000 rpm for 45 minutes (Hettich Mikro 22R). After centrifugation, the supernatants were collected. Under normal circumstances, centrifuged graphene dispersions have concentrations no higher than ~1 mg/mL,[5] far too low to allow the preparation of high volume fraction, drop cast dispersions. Thus, we developed a novel method to dramatically increase the concentration of dispersed graphene. These supernatants were filtered onto a nylon membrane of pore size 0.45 microns (Sterlitech). The membrane was immersed in either 20ml DMF or THF and sonicated in a bath (Branson MT-1510, 80 W) for 60 minutes. The graphene tends to come off the membrane and become re-dispersed in the DMF or THF at relatively high concentrations. The actual concentration can be measured by filtering 1ml of this high concentration solution though a porous membrane and comparing the initial and final membrane weights. Using this method, we have prepared dispersions with concentrations as high as 20 mg/ml.

The PU was purchased from Hydrosize (product code U2-01, average particle size ~3 µm, www.hydrosize.com). The polymer stock solution was produced by drying a Hydrosize PU/Water dispersion at 60 degrees for 72 hours. The resulting solid was then cut up and

portions dissolved in both THF and DMF to obtain two 50mg/ml (PU/THF and PU/DMF) solutions.

The graphene and polymer stock solutions in DMF and THF were blended to create a range of 10 dispersions of varying mass fraction (between 0 and 90 wt%) for both DMF and THF. These dispersions were of constant mass (100mg total of graphene and polymer) and constant volume (5ml total of graphene, polymer and solvent). These samples were sonicated in the same bath as before for 4 hours to homogenise the blended solutions and were then drop cast into 1cm×2cm×2cm Teflon trays. These trays were dried for 12 hours in a vacuum oven (60 degrees at 50 mbar for DMF films and room temp at 900 mbar for THF films to avoid solvent boiling) and further dried at 60 degrees for 72 hours in a normal oven. The films were then removed from the trays and cut into strips of width 2.25mm for tensile testing.

Transmission electron microscopy (TEM) was performed by dropping small quantities of graphene containing dispersions on holey carbon grids using a Jeol 2100, operated at 200kV. An Orion Plus helium ion microscope system was used to image the films. A 5 micron aperture was used for polymer and composite films with a beam current of 0.5pA. Raman spectra were taken using Horiba Jobin Yvon LabRAM-HR with 633nm red laser. Differential scanning calorimetry (DSC) was carried out with a Perkin Elmer Diamond DSC with a heating scan rate of 20 ºC/minute in the temperature range from –45 ºC to 170 ºC. Tensile tests were carried out using a Zwick Roell with a 100 N load cell at a strain rate of 50 mm/min

3.0 Results and Discussion

3.1 Graphene dispersion and composite morphology

We have prepared graphene-PU composite films by drop casting graphene-PU dispersions. These dispersions were prepared using two solvents, THF and DMF, which have low and high boiling points respectively. The aim was to check for solvent effects on the mechanical properties of the composites. It is known that graphene can be dispersed and exfoliated effectively in DMF but not in THF.[3, 4] However, we found that graphene could be exfoliated in THF in the presence of dissolved PU. The exfoliated graphene was reasonably stable with the stabilisation mechanism probably described by partial polymer absorption and steric stabilisation.[29, 30] We analysed the exfoliation state of graphene in DMF (0.1mg/ml), DMF/PU and THF/PU (both 45:55 mass ratio, 0.3mg/ml solid concentration) by TEM. In each case, many few-layer graphene flakes were observed. Typical lateral sizes ranged from 100 nm to 5 μm. Examples are shown in figure 1 A-C. We note that the detailed structure of the PU, in terms of the composition and specific chemistry of the hard and soft segments, is probably important for the graphene stabilisation (and mechanical properties of the resultant composites). Unfortunately the manufacturer declined to provide this information.

We prepared films by drop casting the dispersions into a mould and drying. These were examined using He ion microscopy. Shown in figure 1D&E are He ion images of fracture surfaces of an unfilled PU film and a 55wt% graphene/PU composite. While the fracture surface of the PU film is fairly featureless, the composite film has large numbers of graphitic flakes protruding. It is not possible to tell the aggregation state of the flakes from these images. To investigate this, Raman spectroscopy was carried out on the high graphene content films (55wt%). Typical spectra are shown in figure 1F. These display a moderate disorder band (Raman D:G ratio ~0.5, typical of flake size close to 1 μm).[5] More importantly, they displayed 2D bands (~2600 cm^{-1}) typical of exfoliated graphene with <5

layers per flake.[31] This strongly suggests that the flakes remain well exfoliated on composite formation, even up to mass fractions of 55wt%.

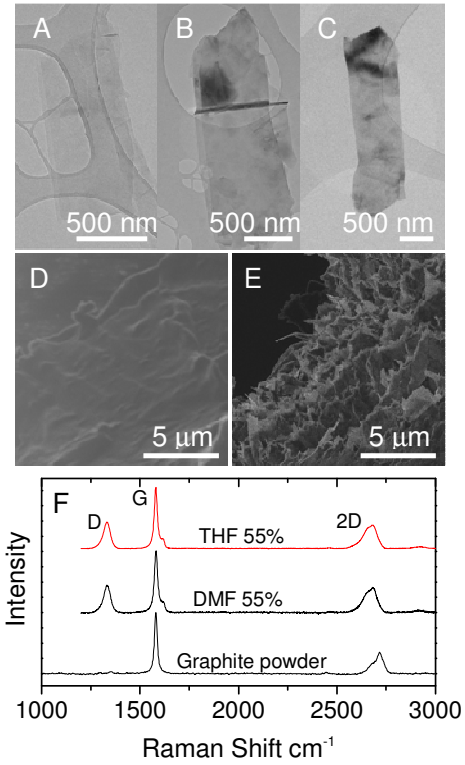

Figure 1: A), B) and C) TEM images of typical graphene flakes dispersed in A) DMF, B) DMF/PU and C) THF/PU. D) Helium ion microscope image of the fracture surface of a PU film. E) He ion image of the fracture surface of a 55wt% graphene PU film (deposited from DMF). F) Raman spectra for graphene-PU composites prepared from both THF and DMF (both 55wt%). Also shown is the spectrum of the starting graphite powder.

We have previously shown that insertion of carbon nanotubes into PU results in changes to the polymer morphology.[24] The PU used here is a thermoplastic elastomer. This is a co-polymer with two different types of chain segments, denoted hard and soft, each with very different properties. The soft segments (SS) have rubber-like properties while the hard

segments tend to form crystallites which act as physical cross-links. The effect is to give PU elastomeric properties. Depending on the nanotube type, nanotube insertion can change the crystallinity of either hard or soft segments in PU.[24] To test the effect of graphene insertion on the PU, we carried out DSC on the PU itself and for composites with 15, 30 and 55wt% graphene (figure S1). The results were similar for both solvents. In the PU films, we observed a single peak at ~25 ^{o}C. A number of researchers have associated this peak with melting of soft segment crystallites.[32-38] For both solvents, we see the reduction in intensity of this peak as graphene content is increased until by 30wt% no SS crystallites are observable. This strongly suggests that the presence of graphene somehow impedes the formation of soft segment crystallites. While the mechanism for this is unclear, we suggest that the graphene interacts strongly, although probably only by van der Waals interactions, with the PU soft segments, hindering motion and so impeding crystallisation.

3.2 The effect of flake size on composite properties

It is known that control of the centrifugation rate allows one to control the lateral size of dispersed graphene flakes.[5] Flake size is likely to influence the mechanical properties of the composites. This makes it critical to test the effect of centrifugation rate on the composite mechanical properties in order to choose an appropriate rotation rate for use in the rest of the study. We prepared graphene-PU composites (20wt%) from dispersions which had been centrifuged at a range of rates from 500 to 1000 rpm. We expect higher rotation rates to result in smaller lateral flake sizes.[5, 39] Representative stress-strain curves are shown in figure S2. It is clear that rotation rate and so flake size significantly affects the mechanical properties. We measured the Young's modulus, Y, the ultimate tensile strength, σ_B, and the strain at break, ε_B, as a function of rotation rate as shown in figure S2 B-D. From this data, it is clear that as rotation rate increases (flake size decreases), Y falls dramatically while σ_B and

ε_B rise slightly. Further work is required to understand these trends. However, we chose to centrifuge at 500 rpm for 45 minutes for the rest of the study as this procedure gives mid-range values of Y, σ_B and ε_B.

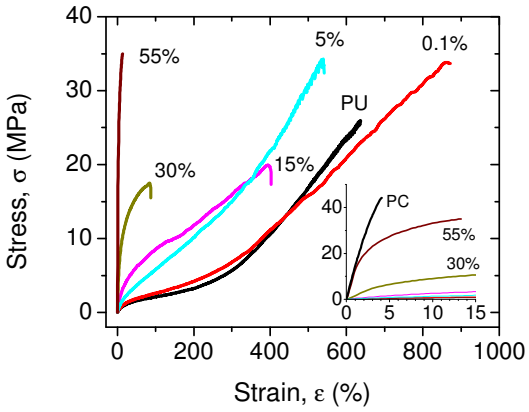

Figure 2: Representative stress-strain curves for polyurethane-graphene composites. While these composites were prepared from DMF, the composites prepared from THF showed vey similar properties. Inset: The low strain region. Note that we have included the stress-strain curve for a solution processed film of polycarbonate (PC) for comparison.

3.3 Mechanical properties as a function of graphene content

We have measured the tensile stress-strain behaviour for graphene-PU composite thin films prepared from both THF and DMF. Representative stress-strain curves for a subset of the composites prepared in DMF are shown in figure 2. The composites prepared in THF show substantially the same behaviour. While the 0.1wt% composite behaves similarly to the PU, composites with higher graphene content show substantially different stress-strain behaviour. As the mass fraction is increased, the stress at a given strain tends to increase steadily. In addition, composites with higher graphene contents tend to fail at lower strain. Shown in the inset of figure 2 is the low strain region of the stress-strain curves. From this

curve it is clear that the 55wt% composite displays significant stress even at low strain. For comparison we have included a stress-strain curve for a solution-cast film of the hard thermoplastic, polycarbonate (PC). We note that for strains below ~1.3% the stress-strain curve for the 55wt% sample is virtually identical to that of PC. At higher strains the 55wt% sample begins to deviate from the PC finally failing at slightly lower stress but much higher strain (PU: σ_B=35 MPa, ε_B=13%, PC: σ_B=44 MPa, ε_B=4%). We emphasize that for some applications, this reduced strength is more than compensated for by the increased ductility and hence toughness.

We can examine the affect of adding graphene in more detail by plotting some specific mechanical properties as a function of graphene content. Shown in figure 3A is Young's modulus plotted as a function of graphene content for both composite types. As with all other mechanical properties, both composite types display almost identical behaviour. This demonstrates that the solvent used during preparation has no real effect on composite properties. This is in contrast carbon nanotube – polyvinylalcohol composites where films prepared from nanotube-dispersing solvents such as N-methylpyrrolidone displayed relatively poor properties compared to more volatile solvents.[40] For graphene-PU composites, the modulus tends to increase exponentially with graphene content before saturating at ~1.5 GPa for mass fractions above 50wt%. We can characterise the exponential rise by the graphene content required to increase Y by a factor of 100. This works out as roughly 45wt%. The dashed line represents the mechanical properties of a solution cast PC film. We see that the composite modulus matches that of this hard thermoplastic for mass fractions above about 45wt%.

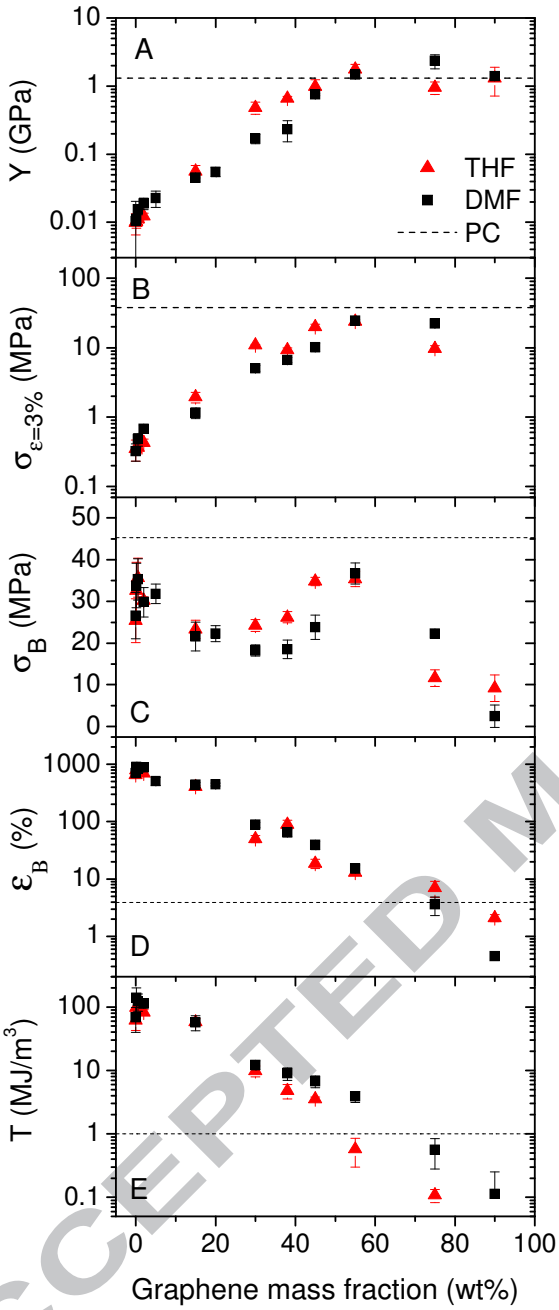

Figure 3: Mechanical properties of graphene–PU composites as a function of graphene content. A) Youngs modulus, B) the stress measured at a strain of 3%, C) the ultimate tensile strength, D) the strain at break and E) the tensile toughness (defined as the area under the

stress –strain curve). In all cases, the dashed line shows the value recorded for polycarbonate processed in a manner equivalent to the PU film.

Although elastomers may be reasonably strong, they generally display large stresses only at high strains. On the contrary, a defining property of hard thermoplastics is the presence of relatively high stress at strains of a few percent. Thus, we measured the stress at a fixed strain of 3% for all our composites. This stress, $\sigma_{\varepsilon=3\%}$, is shown as a function of graphene content in figure 3B. Like the modulus, it increases exponentially before saturating at 25 MPa above 50% strain. This is reasonably close to the value of $\sigma_{\varepsilon=3\%}$=38 MPa measured for polycarbonate. The graphene content required to increase $\sigma_{\varepsilon=3\%}$ by a factor of 100 is ~50wt%.

In figure 3C, we show the ultimate tensile strength, σ_B, as a function of graphene content. The strength shows by far the most complex behaviour as a function of graphene content. Initially, σ_B increases from 25 MPa for PU to 35 MPa for the 0.5wt% composite. As the mass fraction is increased further the strength falls to ~20 MPa at ~30wt%. This behaviour typical for composites and is usually explained by aggregation effects.[16] However, almost identical behaviour was recently observed for composites of polyurethane reinforced with functionalised nanotubes.[24] The reduction in strength was explained in terms of interactions with the PU soft segments resulting in failure at lower stress. A similar phenomenon may be occurring here. The DSC data has shown that the soft segment crystallinity decreases to zero as the graphene content increase to 30wt%. Such disruption of soft segment crystallinity may be responsible for the observed reduction in strength.

However, for graphene content above 30wt%, the strength increases again, reaching 36 MPa for the 55% composite. We note that this is reasonably close to the value of 45 MPa

measured for polycarbonate. The reason for this increase may again be explained by the interaction of the PU soft segments with the graphene. At mass fractions of 30-50wt%, the graphene sheets are on average only nanometers apart. In this scenario, the majority of PU soft segments are likely to be bound to graphene sheets. In this case, the graphene sheets themselves may act like physical cross-links, binding chains together and disrupting chain motion. Such behaviour could conceivably increase the composite strength. However at higher mass factions, the graphene sheets are forced closer together, inevitably resulting in aggregation. If such aggregates are disordered, they may act as stress raisers, weakening the material.

Shown in figure 3D and E are the strain at break, ε_B, and the toughness, T, (defined as the area under the stress-strain curve). Unsurprisingly, both strain at break and toughness fall, apparently exponentially, with increasing mass fraction. This is often observed in nano filled-elastomer composites[20, 21, 23]. The graphene contents required to decrease ε_B and T by a factor of 100 are ~60wt% in each case. We note that for composites with mass fraction up to 75wt%, both ε_B and T are higher than in PC. For lower mass fractions, ε_B and T are dramatically higher. This may give these materials significant advantages over hard thermoplastics in some applications.

We can compare these results to previously published work by Blighe et al on high volume fraction composites of PU filled with Hipco SWNTs.[20] In this paper the mechanical properties of such composites were measured from 0wt% to 100 wt% SWNTs, making direct comparison with the results presented here possible. Blighe observed the modulus to increase linearly with SWNT content, never exceeding 0.5 GPa, significantly worse than the graphene results. In contrast the ultimate tensile strength actually fell on the introduction of nanotubes, hovering between 5 and 10 MPa for all mass fractions. Like the

results presented here, the strain at break fell exponentially with nanotube content, dropping by two orders of magnitude over the first 40 wt% nanotubes. However, in the graphene composites presented here, ε_B fell slower, dropping by two orders of magnitude over the first 60 wt% graphene. Similarly, Blighe observed the toughness to fall exponentially with nanotube content, again dropping by two orders of magnitude over the first 40 wt% nanotubes. However, in the graphene composites, T fell more slowly, dropping by two orders of magnitude over the first 70 wt% graphene. Thus, addition of graphene to PU results in much better mechanical performance than for similar nanotube-based composites.

In order to achieve the original goal of achieving composites with high stiffness and strength yet large ductility and toughness, we said it would be necessary to improve stiffness and strength at a faster rate than ductility and toughness are degraded. We can see that this is the case by examining the mass fractions required to achieve an increase / decrease by a factor of 100 in a given property. For Y, $\sigma_{\varepsilon=3\%}$, ε_B and T, these values were 45, 50, 60 and 60wt% respectively. This shows that Y and $\sigma_{\varepsilon=3\%}$ did indeed increase marginally faster than ε_B and T decreased. As a result, the materials described here share the desirable properties of both rigid thermoplastics and elastomers as shown in table 1. For the 45 and 55 wt% samples the moduli are very close to the PC value. While both $\sigma_{\varepsilon=3\%}$ and σ_B are lower than that of PC, for the 55wt% composite, they come within 35% and 20% respectively. However, the strain at break and toughness for both 45 and 55 wt% composites far exceed those of PC. The 45% composite is 10 times more ductile and 7 times tougher than PC.

Material	Y (GPa)	$\sigma_{\varepsilon=3\%}$ (MPa)	σ_B (MPa)	ε_B (%)	T (MJ/m^3)
PU-graphene, 45wt%	0.75	10	24	40	7
PU-graphene, 55wt%	1.5	25	37	15	4
Solution cast PC	1.3	38	45	4	1

Table 1: Mechanical properties of PU-graphene composites compared to polycarbonate.

While we have prepared composites with high stiffness and strength yet large ductility and toughness, we accept that we have not prepared materials with properties which surpass all common thermoplastics. For example, there are a number of polymers such as polypropylene or polyethylene which are reasonably stiff and strong yet can have high ductility and toughness. However, we propose that the method here could be improved significantly by chemical modification of the graphene or careful choice of the chemical structures of the PU hard soft segments and their mass ratio. By tailoring the interaction of the graphene flakes with the PU it may be possible to obtain the increases in stiffness and stress at low strain while maintaining the ductility and toughness.

4.0 Conclusion

We have prepared high concentration dispersions of graphene stabilised by polyurethane in the solvents tetrahydrofuran and dimethylformamide. This has allowed us to produce graphene/polyurethane composites by drop casting with graphene mass fractions from 0% to 90%. Raman spectroscopy showed the graphene to be well exfoliated, even at mass fractions up to 55wt%. Differential scanning calorimetry showed the PU soft segment crystallite content to fall with increasing graphene content. Addition of graphene resulted in exponential increases in both the Young's modulus and the stress at 3% strain with these quantities saturating at values of 1 GPa and 25 MPa respectively for mass fractions above 50wt%. The ultimate tensile stress showed more complex behaviour but remained between 17 and 40 MPa for all graphene contents below 75wt%. The strain at break and toughness fell exponentially with increasing mass fraction. However, both quantities fell slower with increasing graphene content than the modulus or stress at low strain.

The fact that the low strain properties (Y & $\sigma_{\varepsilon=3\%}$) improved faster than the high strain properties (ε_B & T) is critical. It means that on addition of graphene, the low strain properties can be improved without catastrophic loss of the high strain properties. This means that while graphene / PU composites have properties intermediate to rigid thermoplastics and elastomers, the combination is a potentially useful one. For example, we have prepared a composite (PU-graphene, 55wt%) with Y=1.5 GPa, $\sigma_{\varepsilon=3\%}$=25 MPA, σ_B=37 MPa, ε_B=15% and T=4 MJ/m^3. These values of Y, $\sigma_{\varepsilon=3\%}$ and σ_B are similar to typical thermoplastics. However, ε_B and T are much higher than most rigid thermoplastics. We believe that further optimisation of this method, perhaps by selectively functionalising the graphene sheets to facilitate interaction with the matrix, could result in further improvements. Thus, we believe this method could eventually be used to prepare composites with mechanical properties not found in common polymers.

Acknowledgments

We acknowledge financial support from Science Foundation Ireland through the principle investigator scheme.

Figures Captions

Figure 1: A), B) and C) TEM images of typical graphene flakes dispersed in A) DMF, B) DMF/PU and C) THF/PU. D) Helium ion microscope image of the fracture surface of a PU film. E) He ion image of the fracture surface of a 55wt% graphene PU film (deposited from DMF). F) Raman spectra for graphene-PU composites prepared from both THF and DMF (both 55wt%). Also shown is the spectrum of the starting graphite powder.

Figure 2: Representative stress-strain curves for polyurethane-graphene composites. While these composites were prepared from DMF, the composites prepared from THF showed vey similar properties. Inset: The low strain region. Note that we have included the stress-strain curve for a solution processed film of polycarbonate (PC) for comparison.

Figure 3: Mechanical properties of graphene–PU composites as a function of graphene content. A) Youngs modulus, B) the stress measured at a strain of 3%, C) the ultimate tensile strength, D) the strain at break and E) the tensile toughness (defined as the area under the stress –strain curve). In all cases, the dashed line shows the value recorded for polycarbonate processed in a manner equivalent to the PU film.

Table 1: Mechanical properties of PU-graphene composites compared to polycarbonate

[1] Stankovich S, Dikin DA, Dommett GHB, Kohlhaas KM, Zimney EJ, Stach EA, et al. Graphene-based composite materials. Nature. 2006 Jul;442(7100):282-6.
[2] Stankovich S, Piner RD, Nguyen ST, Ruoff RS. Synthesis and exfoliation of isocyanate-treated graphene oxide nanoplatelets. Carbon. 2006 Dec;44(15):3342-7.
[3] Hernandez Y, Lotya M, Rickard D, Bergin SD, Coleman JN. Measurement of Multicomponent Solubility Parameters for Graphene Facilitates Solvent Discovery. Langmuir. 2010 Mar;26(5):3208-13.
[4] Hernandez Y, Nicolosi V, Lotya M, Blighe FM, Sun ZY, De S, et al. High-yield production of graphene by liquid-phase exfoliation of graphite. Nature Nanotechnology. 2008 Sep;3(9):563-8.
[5] Khan U, O'Neill A, Lotya M, De S, Coleman JN. High-Concentration Solvent Exfoliation of Graphene. Small. 2010;6(7):864-71.
[6] Lee C, Wei XD, Kysar JW, Hone J. Measurement of the elastic properties and intrinsic strength of monolayer graphene. Science. 2008 Jul;321(5887):385-8.
[7] Cai DY, Song M. A simple route to enhance the interface between graphite oxide nanoplatelets and a semi-crystalline polymer for stress transfer. Nanotechnology. 2009 Aug;20(31).
[8] Das B, Prasad KE, Ramamurty U, Rao CNR. Nano-indentation studies on polymer matrix composites reinforced by few-layer graphene. Nanotechnology. 2009 Mar;20(12).
[9] Kim H, Macosko CW. Processing-property relationships of polycarbonate/graphene composites. Polymer. 2009 Jul;50(15):3797-809.
[10] Kim IH, Jeong YG. Polylactide/Exfoliated Graphite Nanocomposites with Enhanced Thermal Stability, Mechanical Modulus, and Electrical Conductivity. Journal of Polymer Science Part B-Polymer Physics. 2010 Apr;48(8):850-8.
[11] Li Q, Li ZJ, Chen MR, Fang Y. Real-Time Study of Graphene's Phase Transition in Polymer Matrices. Nano Letters. 2009 May;9(5):2129-32.
[12] Liang JJ, Huang Y, Zhang L, Wang Y, Ma YF, Guo TY, et al. Molecular-Level Dispersion of Graphene into Poly(vinyl alcohol) and Effective Reinforcement of their Nanocomposites. Advanced Functional Materials. 2009 Jul;19(14):2297-302.
[13] Ramanathan T, Abdala AA, Stankovich S, Dikin DA, Herrera-Alonso M, Piner RD, et al. Functionalized graphene sheets for polymer nanocomposites. Nature Nanotechnology. 2008 Jun;3(6):327-31.
[14] Xu YX, Hong WJ, Bai H, Li C, Shi GQ. Strong and ductile poly(vinyl alcohol)/graphene oxide composite films with a layered structure. Carbon. 2009 Dec;47(15):3538-43.
[15] Zhao X, Zhang QH, Chen DJ, Lu P. Enhanced Mechanical Properties of Graphene-Based Poly(vinyl alcohol) Composites. Macromolecules. 2010 Mar;43(5):2357-63.
[16] Coleman JN, Khan U, Blau WJ, Gun'ko YK. Small but strong: a review of mechanical properties of carbon nanotubes-polymer composites. Carbon. 2006;44:1624-52.
[17] Gong L, Kinloch IA, Young RJ, Riaz I, Jalil R, Novoselov KS. Interfacial Stress Transfer in a Graphene Monolayer Nanocomposite. Advanced Materials. 2010;in press.
[18] Barber AH, Cohen SR, Wagner HD. Measurement of carbon nanotube-polymer interfacial strength. Applied Physics Letters. 2003 Jun;82(23):4140-2.
[19] Coleman JN, Cadek M, Blake R, Nicolosi V, Ryan KP, Belton C, et al. High Performance Nanotube-Reinforced Plastics: Understanding the Mechanism of Strength Increase. Advanced Functional Materials. 2004;14(8):791-8.

[20] Blighe FM, Werner BJ, Coleman JN. Towards tough, yet stiff, composites by filling an elastomer with single-walled nanotubes at very high loading level. Nanotechnology. 2008;19:415709.
[21] Li XD, Gao HS, Scrivens WA, Fei DL, Thakur V, Sutton MA, et al. Structural and mechanical characterization of nanoclay-reinforced agarose nanocomposites. Nanotechnology. 2005 Oct;16(10):2020-9.
[22] Xie L, Kirchberg S, Steuernagel L, Ziegmann G. A mechanism influencing micro injection molded weld lines of hybrid nano filled polypropylene. Microsystem Technologies. 2010;DOI 10.1007/s00542-010-1090-0.
[23] Yang BX, Pramoda KP, Xu GQ, Goh SH. Mechanical reinforcement of polyethylene using polyethylene-grafted multiwalled carbon nanotubes. Advanced Functional Materials. 2007 Sep;17(13):2062-9.
[24] Khan U, Blighe FM, Coleman JN. Selective mechanical reinforcement of thermoplastic polyurethane by targeted insertion of functionalised SWCNTs Journal of Physical Chemistry C. 2010;114(26):11401-8.
[25] Cai DY, Yusoh K, Song M. The mechanical properties and morphology of a graphite oxide nanoplatelet/polyurethane composite. Nanotechnology. 2009 Feb;20(8).
[26] Lee YR, Raghu AV, Jeong HM, Kim BK. Properties of Waterborne Polyurethane/Functionalized Graphene Sheet Nanocomposites Prepared by an in situ Method. Macromolecular Chemistry and Physics. 2009 Aug;210(15):1247-54.
[27] Nguyen DA, Lee YR, Raghu AV, Jeong HM, Shin CM, Kim BK. Morphological and physical properties of a thermoplastic polyurethane reinforced with functionalized graphene sheet. Polymer International. 2009 Apr;58(4):412-7.
[28] Raghu AV, Lee YR, Jeong HM, Shin CM. Preparation and Physical Properties of Waterborne Polyurethane/Functionalized Graphene Sheet Nanocomposites. Macromolecular Chemistry and Physics. 2008 Dec;209(24):2487-93.
[29] Bourlinos AB, Georgakilas V, Zboril R, Steriotis TA, Stubos AK, Trapalis C. Aqueous-phase exfoliation of graphite in the presence of polyvinylpyrrolidone for the production of water-soluble graphenes. Solid State Communications. 2009 Dec;149(47-48):2172-6.
[30] Coleman JN. Liquid-Phase Exfoliation of Nanotubes and Graphene. Advanced Functional Materials. 2009 Dec;19(23):3680-95.
[31] Ferrari AC, Meyer JC, Scardaci V, Casiraghi C, Lazzeri M, Mauri F, et al. Raman spectrum of graphene and graphene layers. Physical Review Letters. 2006 Nov;97(18).
[32] Chen W, Tao X, Liu Y. Carbon nanotube-reinforced polyurethane composite fibers. Composites Science and Technology. 2006;66(15):3029-34.
[33] Jeong HM, Lee JB, Lee SY, Kim BK. Shape memory polyurethane containing mesogenic moiety. Journal of Materials Science. 2000;35(2):279-83.
[34] Koerner H, Kelley JJ, Vaia RA. Transient Microstructure of Low Hard Segment Thermoplastic Polyurethane under Uniaxial Deformation. Macromolecules. 2008;41(13):4709-16.
[35] Koerner H, Liu W, Alexander M, Mirau P, Dowty H, Vaia RA. Deformation-morphology correlations in electrically conductive carbon nanotube--thermoplastic polyurethane nanocomposites. Polymer. 2005;46(12):4405-20.
[36] Koerner H, Price G, Pearce NA, Alexander M, Vaia RA. Remotely actuated polymer nanocomposites[mdash]stress-recovery of carbon-nanotube-filled thermoplastic elastomers. Nature Materials. 2004;3(2):115-20.
[37] Korley LTJ, Pate BD, Thomas EL, Hammond PT. Effect of the degree of soft and hard segment ordering on the morphology and mechanical behavior of semicrystalline segmented polyurethanes. Polymer. 2006;47(9):3073-82.

[38] Yoo HJ, Jung YC, Sahoo NG, Cho JW. Polyurethane-Carbon Nanotube Nanocomposites Prepared by In-Situ Polymerization with Electroactive Shape Memory. Journal of Macromolecular Science, Part B. 2006;45(4):441 - 51.
[39] Lotya M, King PJ, Khan U, De S, Coleman JN. High-Concentration, Surfactant-Stabilized Graphene Dispersions. ACS Nano. 2010;asap.
[40] Khan U, Ryan KP, Blau WJ, Coleman JN. The effect of solvent choice on the mechanical properties of carbon nanotube-polymer composites. Composites Science and Technology. 2007;67(15-16):3158-67.